Fuel 97 (2012) 366–372

Contents lists available at SciVerse ScienceDirect

Fuel

journal homepage: www.elsevier.com/locate/fuel

Synthesis of geopolymer composites from blends of CFBC fly and bottom ashes

Qin Li [a], Hui Xu [a], Feihu Li [b], Peiming Li [a], Lifeng Shen [a], Jianping Zhai [a,*]

[a] State Key Laboratory of Pollution Control and Resource Reuse, School of the Environment, Nanjing University, Nanjing 210093, PR China
[b] School of Environmental Science and Engineering, Nanjing University of Information Science and Technology, Nanjing 210044, PR China

ARTICLE INFO

Article history:
Received 14 July 2011
Received in revised form 22 February 2012
Accepted 22 February 2012
Available online 8 March 2012

Keywords:
CFBC
Fly ash
Bottom ash
Geopolymer
Alkali fusion

ABSTRACT

Blends of circulating fluidized bed combustion (CFBC) fly and bottom ashes of the same coal origin were investigated as raw materials for geopolymer synthesis. Reactivity of the low-reactive CFBC fly ash (CFA) was enhanced by an alkali-fusion pretreatment, which was optimized by an L_{16} (4^4) orthogonal array. It was found that, at a relatively low sodium hydroxide to CFA mass ratio of 0.5, effective alkali fusion could be achieved at 350 °C for 0.5 h. The fused CFA was blended with ground CFBC bottom ash (CBA) at mass ratios of 2.00, 1.00, 0.55, 0.29, and 0.12, and activated by two sodium silicate solutions (21.6 wt% and 34.5 wt%). Geopolymer pastes were cured at 40 °C for 7 days, reaching a highest compressive strength of 34.0 MPa. Characterization of the raw materials and geopolymer products was also conducted by an alkaline dissolution test, thermogravimetric–differential thermal analysis (TG–DTA), X-ray diffractography (XRD), scanning electron microscopy (SEM), as well as Fourier transform infrared spectroscopy (FTIR). The results of this study suggest that, by a moderate alkali-fusion pretreatment at temperatures slightly higher than the melting point for sodium hydroxide (318 °C), low-reactive CFA can be recycled together with CBA for production of value-added geopolymer composites.

1. Introduction

Circulating fluidized bed combustion (CFBC) is an advanced and mature solution for clean, reliable and economic coal combustion technology, which has met the environmental requirements for large reductions in NO_x and SO_2 releases from coal-fired power plants [1–3]. While conventional pulverized coal combustion (PCC) is typically operated at high temperatures in the range of 1300–1700 °C [4], CFBC features a remarkably lowered temperature of ca. 850 °C and thus significantly reduces NO_x emissions [5]. Besides, CFBC is particularly well suited for in situ SO_2 removal by use of limestone without significant grinding or processing [6]. Other notable advantages of CFBC include suitability for CO_2 capture by CaO-based sorbants, high combustion efficiency, as well as wide fuel flexibility [3,7,8]. Consequently, CFBC has grown steadily all over the world ever since its commercialization in the 1970s and has become the most common fluidized combustion design [9]. In China, more than 1000 CFBC boilers are currently in operation, with others in construction or design phases [10].

However, the resulting CFBC fly ash (CFA) and bottom ash (CBA) have posed severe challenges to both the government and power plants [11,12]. Mainly due to its unique thermal history, CFA differs distinctly from typical PCC fly ash (PFA) in physical and chemical characteristics [13,14]. Generally, the majority of PFA can be recycled in construction materials, such as cement and concrete. This is due to its high SiO_2 and Al_2O_3 contents as well as the pozzolanic property after reacting with lime and water [15,16]. However, this is not the case for CFA, which meets neither North American nor European standards for components or additives in concretes [17]. In spite of the cementitious properties [18], the use of CFA in concretes may lead to structural damage and strength reduction due to the presence of free lime, relatively low SiO_2 and Al_2O_3 contents, large specific surface area, high water requirement, as well as harmful pores [3,17,19]. Even landfill disposal of CFA is difficult because of the highly exothermic reaction with water, high-pH leachate, and excessive expansion of solidified material [20]. Moreover, the significantly lowered firing temperature results in almost no reactive vitreous content, making CFA an unfavorable raw material for direct geopolymer synthesis [12].

Geopolymers are a class of synthetic aluminosilicate inorganic polymers (AIPs) featuring a predominantly X-ray amorphous three-dimensional network [21,22]. The fundamental nanostructure of geopolymers consists of tetrahedral coordination of Si and Al linked by oxygen bridges, with alkalis cations (typically Na^+ and/or K^+) associated for balancing the negative charges on tetrahedral Al sites [23]. Based on such a unique structure, geopolymers may exhibit superior mechanical, chemical and thermal properties in comparison with ordinary Portland cement (OPC) [24], making them a promising alternative for a variety of applications, such as new ceramics and cements, matrices for hazardous waste stabilization, toolings and moldings, fire-resistant materials and high-tech

* Corresponding author. Tel.: +86 25 8359 2903.
E-mail address: jpzhai@nju.edu.cn (J. Zhai).

0016-2361/$ - see front matter © 2012 Elsevier Ltd. All rights reserved.
doi:10.1016/j.fuel.2012.02.059

materials [25,26]. In addition, when compared with traditional OPC, geopolymers can generally deliver an 80% or greater reduction in CO_2 footprint and require roughly 60% less energy. Thus geopolymers can be regarded as a 'green concrete' [26,27].

Due to the significant environmental benefits as well as sound properties of coal ash-based geopolymer products, recycling of fly and bottom ashes by geopolymer technology has drawn great interest [28–30]. However, to the authors' best knowledge, no geopolymerization of sole CFA has ever been reported, possibly due to the low reactivity of CFA. Although an alkali-fusion process was introduced to enhance the reactivity of CFA for geopolymer synthesis [12], the extremely high Na/Al ratio had to be balanced by a large volume of metakaolin, which was derived from the calcination of a natural kaolinitic resource at 500–750 °C for several hours [25]. Besides, the alkali fusion formerly reported at 550 °C for 2.0 h has not been optimized for geopolymer applications [12]. Moreover, synthesis of geopolymers from blends of the alkali-fused CFA (f-CFA) and metakaolin makes no use of the accompanying by-product CBA, which may possess high reactive Si and Al contents and also requires recycling and/or landfill disposal [11].

This study, therefore, investigated synthesis and characterization of geopolymers from blends of f-CFA and ground CBA (g-CBA) with no natural kaolinitic resource involved. Reactivity of the CFA was enhanced by a moderate alkali-fusion pretreatment, which was assessed by an alkaline-dissolution test [31] and optimized by an L_{16} (4^4) orthogonal array. Sample characterizations were performed by mechanical strength test, thermogravimetric–differential thermal analysis (TG–DTA), X-ray diffractography (XRD), scanning electron microscopy (SEM), as well as Fourier transform infrared spectroscopy (FTIR).

2. Experimental procedures

2.1. Materials

CFBC fly and bottom ashes, collected from Sinopec Jinling Petrochemical Power Plant (Nanjing, China), are of the same origin from a Chinese soft coal. The as-received CBA, consisting of slag-like particles of different sizes (up to 20 mm), was ground in a laboratory ball mill prior to geopolymerization. Particle size distributions of the raw CFA (r-CFA) and g-CBA were determined by a Mastersizer 2000 laser analyzer (Malvern, UK) and the results are shown in Fig. 1. Chemical compositions of the CFA and CBA, as determined on a 9800XP$^+$ X-ray fluorescence spectrometer (XRF) (ARL, Switzerland), are presented in Table 1. Both of the ashes contain trace amounts of toxic heavy metals and hazardous elements, which may pose potential threats to the environment if not properly disposed.

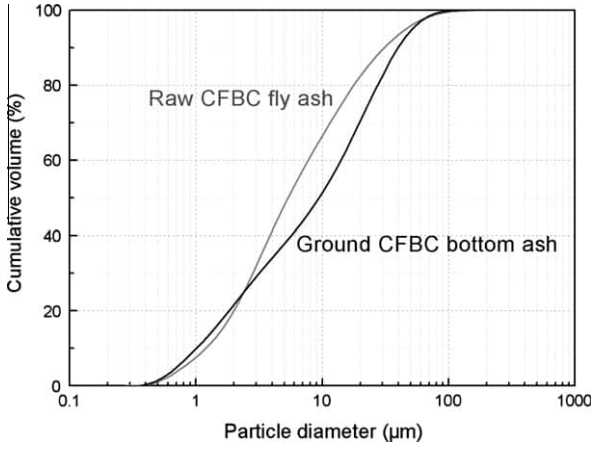

Fig. 1. Particle size distributions of raw CFBC fly ash and ground CFBC bottom ash.

Analytical grade sodium hydroxide was used for the alkali-fusion pretreatment of CFA. An industrial grade sodium silicate, consisting of 60.3 wt% SiO_2 and 26.0 wt% Na_2O, was employed for preparation of two alkaline activating solutions of different concentrations. All experiments were performed using the same batches of raw materials and chemicals and deionized water was used throughout.

2.2. Alkali fusion

Reactivity of the low-reactive CFA was enhanced by alkali fusion of the ash with sodium hydroxide pellets. An L_{16} (4^4) orthogonal array was designed for optimization of the fusion process, focusing on four primary factors, i.e., NaOH/CFA ratio, temperature, time and heating rate. Effect of combinations of the factors and levels on the alkali fusion was assessed by dissolution extents of Si and Al form the f-CFA in alkaline solutions [31]. The dissolution test was conducted at room temperature by mixing 0.500 ± 0.002 g of CFA with 20.0 ml of 5.00 M NaOH solution for 5 h using a magnetic stirrer. An Optima 5300DV inductively coupled plasma optical emission spectrometer (ICP-OES) (Perkin Elmer, USA) was employed for analysis of the dissolved Si and Al contents.

2.3. Geopolymer preparation

Geopolymer samples were synthesized by alkaline-activation of a series of blends of f-CFAs and g-CBA, at mass ratios of 2.00, 1.00, 0.55, 0.29 and 0.12, with two silicate solutions (solution A of 21.6 wt% silicate and solution B of 34.5 wt% silicate). The liquid/solid (L/S) mass ratios were kept in the range of 0.57–0.87, depending on an acceptable workability for each paste sample. It should be noted that the activator liquid contained 34.5 wt% or 21.6 wt% of solid sodium silicate. Therefore, the actual water to solid (W/S) ratios are 0.40–0.51 for samples with solution A and 0.37–0.44 for samples with solution B. Table 2 presents the mix designs for all geopolymer samples. The sample ID in Table 2 consists of activator solution concentration (A for 21.6 wt% and B for 34.5 wt%), fusion temperature (550 or 350 °C), as well as f-CFA/CBA mass ratio (1, 2, 3, 4 and 5 for 2.00, 1.00, 0.55, 0.29 and 0.12, respectively).

Fresh geopolymer pastes were cast in triplet steel molds of 20-mm cubes and vibrated for 5 min to remove entrained air bubbles. The molds were then sealed with polyethylene film and set into a standard curing box. After initial curing at 40 °C for 24 h, the samples were demolded and subjected to further curing at 40 °C for 144 h.

2.4. Sample analysis

Compressive strength test was performed immediately after the 7-day curing had finished, using an NYL-300 compressive strength testing apparatus (Wuxi Jianyi, China). For selected geopolymer samples, simultaneous TG–DTA was conducted from 25 to 1000 °C at a heating rate of 10 °C per minute on an STA 449C thermal analyzer (Netzsch, Germany). SEM photomicrographs were obtained on an S-3400N scanning electron microscope (Hitachi, Japan), and XRD patterns were recorded by an X'TRA high-performance powder X-ray diffractometer (ARL, Switzerland) with Cu Kα radiation generated at 40 mA and 40 kV. A Nicolet 6700 FTIR spectrometer (Thermo Scientific, USA) was employed for the collection of the FTIR data, using KBr pressed disk method.

Table 1
Chemical compositions of CFBC fly and bottom ashes.

	SiO_2	Al_2O_3	CaO	Fe_2O_3	TiO_2	Na_2O	K_2O	MgO	MnO	SO_3	P_2O_5	LOI[a]
Major elements as oxide of CFBC fly and bottom ashes (wt%)												
CFA	43.42	28.53	14.06	3.01	1.47	0.18	0.84	0.28	0.02	2.66	0.12	5.03
CBA	61.17	26.78	2.05	4.35	0.95	0.34	1.54	0.61	0.05	0.09	0.07	1.69
	Ba	Zr	Sr	V	Cr	Zn	Rb	Cu	Ni	Ga	Pb	Y
Trace element contents of CFBC fly and bottom ashes (μg/g)												
CFA	965.5	211.4	474.2	369.4	142.6	60.8	21.8	67.5	69.5	0.0	0.0	39.6
CBA	408.2	217.3	190.9	118.4	143.0	66.8	74.1	62.6	47.7	31.8	24.7	22.4

[a] LOI, loss on ignition at 960 °C.

Table 2
Mix designs and calculated molar ratios for geopolymer composites.

Geopolymer	Concentration of sodium silicate solution (wt%)	F-CFAs/CBAs (mass ratio)	Liquid/solid (mass ratio)	Si/Al	Na/Al	H_2O/Na
A550-1	21.6	2.00	0.76	1.88	1.96	3.98
A550-2	21.6	1.00	0.70	1.95	1.50	4.54
A550-3	21.6	0.55	0.64	2.00	1.13	5.26
A550-4	21.6	0.29	0.61	2.08	0.84	6.45
A550-5	21.6	0.12	0.57	2.22	0.59	8.24
A350-1	21.6	2.00	0.76	1.88	1.96	3.98
A350-2	21.6	1.00	0.70	1.95	1.50	4.54
A350-3	21.6	0.55	0.64	2.00	1.13	5.26
A350-4	21.6	0.29	0.61	2.08	0.84	6.45
A350-5	21.6	0.12	0.57	2.22	0.59	8.24
B550-1	34.5	2.00	0.87	2.14	2.49	3.01
B550-2	34.5	1.00	0.84	2.20	2.00	3.40
B550-3	34.5	0.55	0.82	2.25	1.63	3.88
B550-4	34.5	0.29	0.76	2.30	1.28	4.42
B550-5	34.5	0.12	0.71	2.41	0.98	5.15
B350-1	34.5	2.00	0.87	2.14	2.49	3.01
B350-2	34.5	1.00	0.84	2.20	2.00	3.40
B350-3	34.5	0.55	0.82	2.25	1.63	3.88
B350-4	34.5	0.29	0.76	2.30	1.28	4.42
B350-5	34.5	0.12	0.71	2.41	0.98	5.15

3. Results and discussion

3.1. Effect and optimization of alkali fusion

Geopolymerization is believed to be a complex multiphase process which includes a series of dissolution, reorientation and solidification reactions [32]. Hence, dissolution of Si and Al species from solid sources under alkaline conditions plays a significant role on reactivity of a raw material for geopolymerization [12,33].

On the other hand, alkali fusion is a general method with a long history for decomposing materials containing Si and Al in chemical analysis [34]. In this study, alkali-fusion process was optimized by an L_{16} (4^4) orthogonal array, as detailed in Tables 3 and 4, and employed as a pretreatment for enhancing reactivity of the low-reactive CFA. The effect of alkali fusion was assessed by a dissolution test in alkaline solutions [31]. For f-CFA samples of different alkali/ash ratios, the masses of the f-CFAs and concentrations of the sodium hydroxide solutions were regulated to keep a constant net CFA weight of 0.500 ± 0.002 g and a fixed sodium concentration of 5.00 M.

Table 3
Factors and levels for L_{16} (4^4) orthogonal array.

Factor	Level			
	1	2	3	4
A. NaOH/CFA mass ratio	0.30	0.40	0.50	0.60
B. Heating temperature (°C)	350	450	550	650
C. Heating duration (min)	30	60	90	120
D. Heating rate (°C/min)	3.0	6.0	9.0	12.0

Analysis of the orthogonal array data suggests $A_4B_1C_1D_4$, i.e., level 4 of factor A, levels 1 of factors B and C, and level 4 of factor D, as the optimal combination of factors and levels. However, highest alkali content results in highest Na/Al ratio to be balanced by g-CBA, and thus utilize less CFA in the geopolymer composite. Therefore, the combination of $A_3B_1C_1D_4$ was recommended in this study. $A_3B_3C_4D_4$, as reported in previous work [12], was also examined for comparison purpose.

The dissolution extents of Si and Al from the CFA, before and after the alkali-fusion treatments, are presented in Table 5. For the recommended combination of $A_3B_1C_1D_4$, the dissolution extents of Si and Al significantly increased 7.9 and 12.6 times, respectively. Although the testing conditions for the raw and alkali-fused CFAs were not exactly the same, the results of this dissolution test suggest that the geopolymerization reactivity of the CFA can be effectively enhanced by the alkali-fusion treatment. In Section 3.3 (X-ray diffractography) of this article, the effect of the alkali fusion on reactivity of the CFA will be further discussed.

3.2. Compressive strength

All geopolymer samples were subjected to compressive strength test after curing at 40 °C for 7 days, and the results are summarized in Fig. 2. As shown in Fig. 2, for activating solution A (21.6 wt% silicate), the compressive strengths of the $A_3B_1C_1D_4$ samples ranged from 8.1 to 12.9 MPa, whereas for activating solution B (34.5 wt% silicate), the compressive strengths were in the range of 21.7–32.7 MPa. It was found that both the f-CFA/CBA ratio and concentration of activating solution may exert significant

Table 4
L_{16} (4^4) orthogonal array for optimization of alkali fusion process.

Test no.	A	B	C	D	Dissolution (ppm)	
	NaOH/CFA mass ratio	Heating temperature (°C)	Heating duration (min)	Heating rate (°C/min)	Al	Si
1	1	1	1	1	853	1275
2	1	2	2	2	523	823
3	1	3	3	3	498	670
4	1	4	4	4	635	763
5	2	1	2	3	1170	1548
6	2	2	1	4	1008	1350
7	2	3	4	1	833	1090
8	2	4	3	2	1058	1090
9	3	1	3	4	1550	1943
10	3	2	4	3	1418	1883
11	3	3	1	2	1283	1780
12	3	4	2	1	1395	1488
13	4	1	4	2	1740	2003
14	4	2	3	1	1913	2330
15	4	3	2	4	2013	2085
16	4	4	1	3	1853	1793

Table 5
Alkaline dissolution extents of Si and Al for selected combinations of factors and levels.

Combination	Si (ppm)	Al (ppm)
$A_4B_1C_1D_4$[a]	2019	1706
$A_3B_1C_1D_4$[b]	1833	1255
$A_3B_3C_4D_4$[b]	1920	1143
Raw CFA[c]	243	100

[a] A 0.800 g of fused CFBC fly ash in 20.0 ml of 4.63 M NaOH solution.
[b] A 0.750 g of fused CFBC fly ash in 20.0 ml of 4.69 M NaOH solution.
[c] A 0.500 g of raw CFBC fly ash in 20.0 ml of 5.00 M NaOH solution.

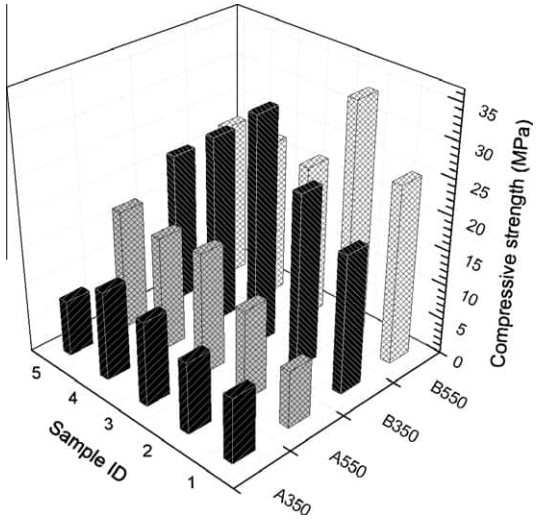

Fig. 2. Compressive strength of geopolymer samples.

effects on the mechanical properties of the CFBC fly and bottom ashes based geopolymers. Apparently, activating solution B with higher concentrations of SiO_2 and Na_2O led to higher compressive strength than solution A did, suggesting that to some extents more soluble Si in the activating solution is favorable for compressive strength development [11]. In this study, geopolymer sample B350-3 reached a reasonably high 7-day compressive strength of 32.7 MPa, which is only slightly lower than the highest 34.0 MPa for sample B550-2. The high strength of geopolymer B350-3 compared to that of A350-4 will be further discussed in Section 3.5 (electron microscopy) of this article.

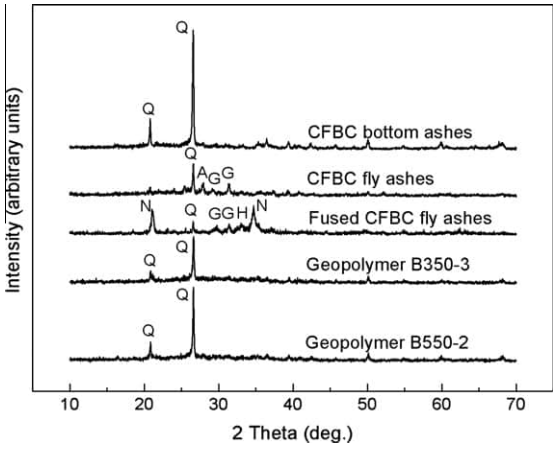

Fig. 3. X-ray diffraction patterns of CFBC bottom ash, raw and alkali-fused CFBC fly ashes, and selected geopolymer samples. Q – quartz (SiO_2), N – nepheline ($NaAlSiO_4$), A – anorthite ($CaAl_2Si_2O_8$), G – gehlenite ($Ca_2Al_2SiO_7$), and H – hematite (Fe_2O_3).

3.3. X-ray diffractography

Fig. 3 shows the XDR patterns of the CBA, raw and alkali-fused CFAs, as well as selected geopolymer samples. It can be seen that the major crystalline phases of both CFBC fly and bottom ashes are exclusively quartz. In the f-CFA, the intensity of quartz phase decreased remarkably, whereas a new crystalline phase of nepheline ($NaAlSiO_4$) formed [12], indicating that a significant amount of quartz in the r-CFA had reacted with sodium hydroxide during the fusion process. As a consequence, the dissolution extents of Si and Al species from the f-CFAs in alkaline aqueous solutions were greatly enhanced due to the formation of the sodium aluminosilicate [35], which has been confirmed by the experimental data presented in Table 5. It is also shown in Fig. 3 that the XRD patterns of the selected geopolymer samples are much similar and the only major crystalline phase is unreacted quartz. By comparing the XRD patterns of the geopolymer products with those of the CFBC fly and bottom ashes, it is evident that no substantial new crystalline phases formed in the geopolymerization process.

3.4. TG–DTA analysis

The TG–DTA and DTG (the first derivative of the residual mass versus temperature) data from room temperature to 1000 °C for

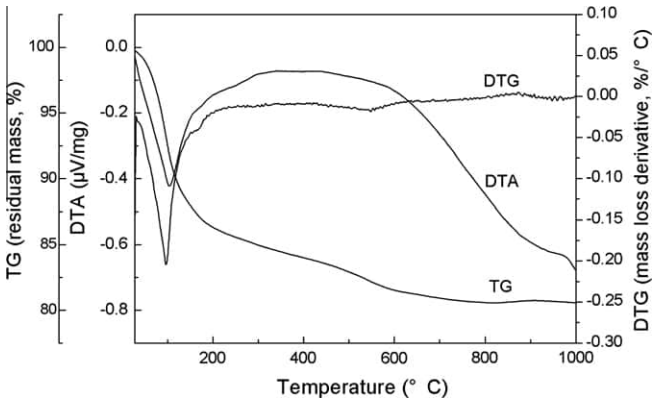

Fig. 4. Thermogravimetric-differential thermal analysis curves of selected geopolymer B350-3.

the selected geopolymer sample B350-3 are presented in Fig. 4. It can be seen from the TG curve that a 19% mass loss occurred over the testing temperature range, implying that the geopolymer sample retained about 19% water after curing at 40 °C for 7 days, of which 8.5% was lost at temperatures below 110 °C. The remainder was either bound tightly or less able to diffuse to the geopolymer surface [36], which continued to evolve at higher temperatures in a dehydration reaction [37], and was lost as gaseous H_2O according to

$$2Si{-}OH \rightarrow Si{-}O{-}Si + H_2O\ (\uparrow) \quad (1)$$

The DTA curve gives a single endothermic peak at about 100 °C due to dehydration (water evolution), which is typical for a geopolymer and differs from those for OPC [36]. It is known that the DTA curves for OPC normally show two endothermic peaks around 135 and 500 °C, which are attributed to the water loss and $Ca(OH)_2$ decomposition, respectively [36,38].

3.5. Electron microscopy

The SEM images of the g-CBA, r-CFA, as well as selected geopolymer samples are shown in Fig. 5. Fig. 5a and b presents the appearances of g-CBA and r-CFA which are quite different from those of conventional PFAs. While typical PFAs largely contain small vitreous spheres, the g-CBA and r-CFA consist exclusively of irregular slag-like particles of different sizes. This may be attributed to the significant differences between the thermal histories with which the PFAs and CFBC ashes are formed. As shown in Fig. 5c and e, samples A550-3 and A350-4 reveal similar substantial, yet less compact, geopolymer structures. On the contrary, Fig. 5d and f presents well-formed homogenous geopolymer matrices for the samples B550-2 and B350-3, indicating that geopolymerization of blend of CFBC fly and bottom ashes with no addition of natural kaolinitic resources can be achieved. Besides, by comparing Fig. 5e with f, it is reasonable to suggest that geopolymer B350-3 may develop a higher compressive strength than

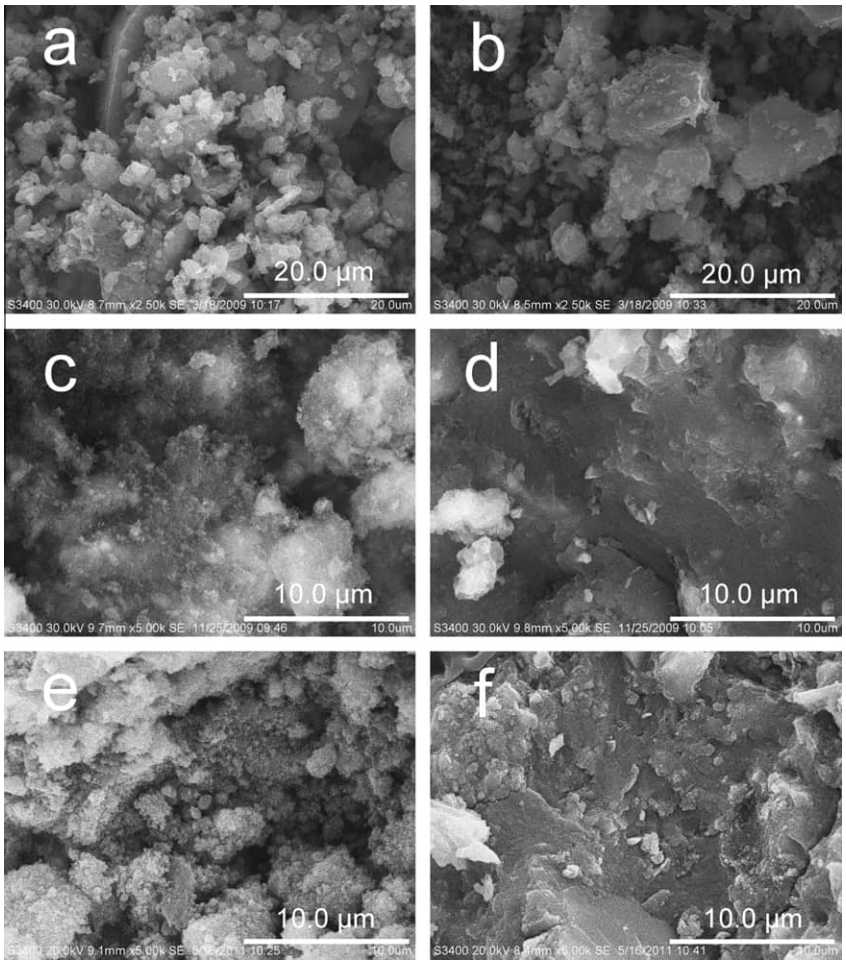

Fig. 5. Scanning electron microscope images of (a) raw CFBC fly ash; (b) ground CFBC Bottom ash; (c) geopolymer A550-3; (d) geopolymer B550-2; (e) geopolymer A350-4; and (f) geopolymer B350-3.

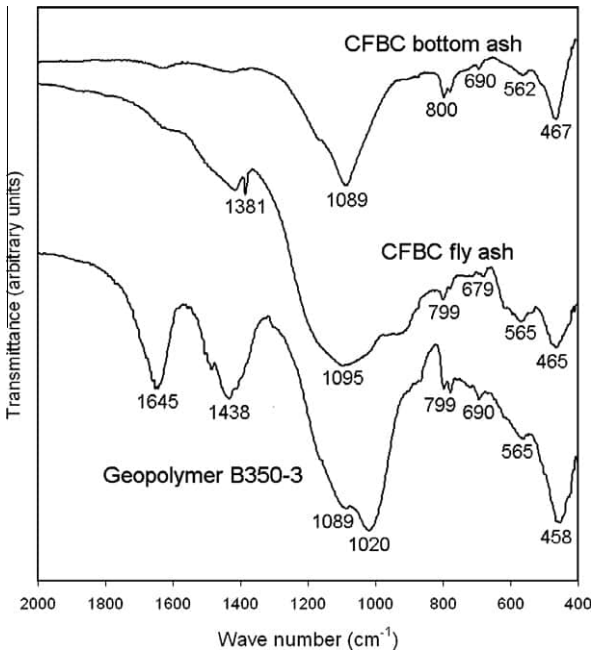

Fig. 6. Infrared spectra of CFBC fly and bottom ashes as well as selected geopolymer sample.

geopolymer A350-4, which is supported by the results of compressive strength testing (Section 3.2) in this study.

3.6. Infrared spectroscopy

FTIR spectroscopy allows identification of different types of chemical bonds in materials on a molecular level. Therefore, the differences between the FTIR absorption frequencies for the source materials and geopolymer products may provide some evidences on effective geopolymerization. Fig. 6 presents the FTIR spectra of the CFBC fly and bottom ashes as well as the selected geopolymer sample B350-3. As shown in the figure, the main features of all FTIR spectra are the prominent bands between 1020 and 1095 cm^{-1}. The bands at 1095 cm^{-1} and 1089 cm^{-1} in the spectra of the CFBC fly and bottom ashes are attributed to the Si–O–Si asymmetric stretching in tetrahedra [39,40], which shifted to a lower frequency of 1020 cm^{-1} for Si–O–Al asymmetric stretching as a consequence of polycondensation with alternating Si–O and Al–O bonds [28]. Other evidence related to geopolymerization may include the band around 1645 cm^{-1} for H–O–H bending vibration [28,39], which is absent in the spectra of the CFA and the CBA. The small bands at approximate 800 and 680 cm^{-1} represent the symmetric Al–O stretching of tetrahedral aluminum and the functional group of AlO_2, respectively [41,42]. The bands at 562–565 cm^{-1} indicate the presence of Al in octahedral coordination [43], whereas those around 465 cm^{-1} are linked to the Si–O–Si and O–Si–O bending modes [29,39]. For the NaOH-rich geopolymer, the common atmospheric carbonation is revealed by the band centered at 1438 cm^{-1} for O–C–O stretching vibration [39].

4. Conclusions

Successful geopolymerization of blends of alkali-fused CFA and ground CBA was achieved in this work. The results of the L_{16} (4^4) orthogonal array study indicate that, the reactivity of low-reactive CFA can be effectively enhanced by a moderate alkali fusion process at a relatively low alkali/ash mass ratio of 0.50 and a greatly lowered heating temperature of 350 °C. In addition, the heating duration can also be shortened from 2.0 h to 0.5 h. The excess alkali in the fused CFA can be consumed by the ground CBA instead of calcined natural kaolin (metakaolin). It is found that both the fused CFA to ground CBA mass ratio and the concentration of alkaline activating solution play significant roles in geopolymerization. The optimal geopolymer sample reached a reasonably high 7-day compressive strength of 32.7 MPa. The method discussed in this study may provide a viable approach to simultaneous and/or in situ massive recycling of both CFBC fly and bottom ashes for production of value-added geopolymer composites.

Acknowledgements

This work was funded by the Natural Science Foundation of China (Grant No. 51008154), the Jiangsu Natural Science Foundation (Grant No. SBK201022682), the Research Fund for the Doctoral Program of Higher Education of China (Grant No. 20090091120007), the Fundamental Research Funds for the Central Universities (Grant No. 1112021101), Larry Syltebo and Kevin Izzo at Vitreous State Laboratory, the Catholic University of America, are gratefully appreciated for language editing support.

References

[1] Manovic V, Anthony EJ. CaO-based pellets supported by calcium aluminate cements for high-temperature CO_2 capture. Environ Sci Technol 2009;43:7117–22.
[2] Anthony EJ, Jia L, Wu Y. CFBC ash hydration studies. Fuel 2005;84:1393–7.
[3] Fu X, Li Q, Zhai J, Sheng G, Li F. The physical-chemical characterization of mechanically-treated CFBC fly ash. Cem Concr Compos 2008;30:220–6.
[4] Chindaprasirt P, Rattanasak U. Utilization of blended fluidized bed combustion (FBC) ash and pulverized coal combustion (PCC) fly ash in geopolymers. Waste Manage 2010;30:667–72.
[5] Li F, Zhai J, Fu X, Sheng G. Characterization of fly ashes from circulating fluidized bed combustion (CFBC) boilers cofiring coal and petroleum coke. Energy Fuel 2006;20:1411–7.
[6] Stewart MC, Manovic V, Anthony EJ, Macchi A. Enhancement of indirect sulphation of limestone by steam addition. Environ Sci Technol 2010;44:8781–6.
[7] Manovic V, Anthony EJ. Competition of sulphation and carbonation reactions during looping cycles for CO_2 capture by CaO-based sorbents. J Phys Chem A 2010;114:3997–4002.
[8] Li F, Li Q, Zhai J, Sheng G. Effect of zeolitization of CFBC fly ash on immobilization of Cu^{2+}, Pb^{2+}, and Cr^{3+}. Ind Eng Chem Res 2007;46:7087–95.
[9] Li Q, Xu H, Fu X, Chen C, Zhai J. Effects of circulating fluidized bed combustion (CFBC) fly ashes as filler on the performances of asphalt. Asia Pac J Chem Eng 2009;4:226–35.
[10] Xiao X, Yang H, Zhang H, Lu J, Yue G. Research on carbon content in fly ash from circulating fluidized bed boilers. Energy Fuel 2005;19:1520–5.
[11] Xu H, Li Q, Shen L, Wang W, Zhai J. Synthesis of thermostable geopolymer from circulating fluidized bed combustion (CFBC) bottom ashes. J Hazard Mater 2010;175:198–204.
[12] Xu H, Li Q, Shen L, Zhang M, Zhai J. Low-reactive circulating fluidized bed combustion (CFBC) fly ashes as source material for geopolymer synthesis. Waste Manage 2010;30:57–62.
[13] Hall ML, Livingston WR. Fly ash quality, past, present and future, and the effect of ash on the development of novel products. J Chem Technol Biotechnol 2002;77:234–9.
[14] Lecuyer I, Bicocchi S, Ausset P, Lefevre R. Physico-chemical characterization and leaching of desulphurization coal fly ash. Waste Manage Res 1996;14:15–28.
[15] Haynes RJ. Reclamation and revegetation of fly ash disposal sites – challenges and research needs. J Environ Manage 2009;90:43–53.
[16] Rubio B, Izquierdo MT, Mayoral MC, Bona MT, Martínez-Tarazona RM. Preparation and characterization of carbon-enriched coal fly ash. J Environ Manage 2008;88:1562–70.
[17] Blondin J, Anthony EJ. A selective hydration treatment to enhance the utilization of CFBC Ash in concrete. In: 13th International conference on FBC, ASME, Orlando; 7–10 May, 1995.
[18] Sheng G, Li Q, Zhai J, Li F. Self-cementitious properties of fly ashes from CFBC boilers co-firing coal and high-sulphur petroleum coke. Cem Concr Res 2007;37:871–6.
[19] Neville AM. Properties of concrete. 3rd ed. London: ELBS with Longman; 1981. p. 257–79.
[20] Anthony EJ, Berry EE, Blondin J, Bulewicz EM, Burwell S. Advanced ash management technologies for CFBC ash. Waste Manage 2003;23:503–16.
[21] Davidovits J. Mineral polymers and methods of making them. US Patent 1982, 4, 349, 386.

[22] Provis JL, van Deventer JSJ. Geopolymerisation kinetics. 1. In situ energy-dispersive X-ray diffractometry. Chem Eng Sci 2007;62:2309–17.
[23] Duxson P, Fernández-Jiménez A, Provis JL, Lukey GC, Palomo A, van Deventer JSJ. Geopolymer technology: the current state of the art. J Mater Sci 2007;42:2917–33.
[24] Rees CA, Provis JL, Lukey GC, van Deventer JSJ. The mechanism of geopolymer gel formation investigated through seeded nucleation. Colloid Surf A 2008;318:97–105.
[25] Cioffi R, Maffucci L, Santoro L. Optimization of geopolymer synthesis by calcination and polycondensation of a kaolinitic residue. Resour Conserv Recy 2003;40:27–38.
[26] Komnitsas K, Zaharaki D. Geopolymerisation: a review and prospects for the minerals industry. Miner Eng 2007;20:1261–77.
[27] Duxson P, Provis JL, Lukey GC, van Deventer JSJ. The role of inorganic polymer technology in the development of 'green concrete'. Cem Concr Res 2007;37:1590–7.
[28] Andini S, Cioffi R, Colangelo F, Grieco T, Montagnaro F, Santoro L. Coal fly ash as raw material for the manufacture of geopolymer-based products. Waste Manage 2008;28:416–23.
[29] Chindaprasirt P, Jaturapitakkul C, Chalee W, Rattanasak U. Comparative study on the characteristics of fly ash and bottom ash geopolymers. Waste Manage 2009;29:539–43.
[30] Somna K, Jaturapitakkul C, Kajitvichyanukul P, Chindaprasirt P. NaOH-activated ground fly ash geopolymer cured at ambient temperature. Fuel 2011;90:2118–24.
[31] Xu H, van Deventer JSJ. The geopolymerisation of alumino-silicate minerals. Int J Miner Process 2000;59:247–66.
[32] Provis JL, Duxson P, van Deventer JSJ, Lukey GC. The role of mathematical modelling and gel chemistry in advancing geopolymer technology. Chem Eng Res Des 2005;83:853–60.
[33] Chen C, Gong W, Lutze W, Pegg IL. Kinetics of fly ash geopolymerization. J Mater Sci 2011;46:3073–83.
[34] Hillebrand WF, Lundell GEF, Bright HA, Hoffman JI. Applied inorganic analysis. 2nd ed. New York: Wiley; 1962.
[35] Chang HL, Shih WH. A general method for the conversion of fly ash into zeolites as ion exchangers for cesium. Ind Eng Chem Res 1998;37:71–8.
[36] Subaer, van Riessen A. Thermo-mechanical and microstructural characterisation of sodium-poly(sialate-siloxo) (Na-PSS) geopolymers. J Mater Sci 2007;42:3117–23.
[37] Lyon RE, Balaguru PN, Foden A, Sorathia U, Davidovits J. Fire-resistant aluminosilicate composites. Fire Mater 1997;21:67–73.
[38] Silva FJ, Mathias AF, Thaumaturgo C. In: Proceedings of Geopolymere'99. Saint-Quentine, France; 1999. p. 97.
[39] Lee WKW, van Deventer JSJ. The effects of inorganic salt contamination on the strength and durability of geopolymers. Colloid Surf A 2002;211:115–26.
[40] Simonsen ME, Sønderby C, Li Z, Søgaard EG. XPS and FT-IR investigation of silicate polymers. J Mater Sci 2009;44:2079–88.
[41] Bakharev T. Geopolymeric materials prepared using Class F fly ash and elevated temperature curing. Cem Concr Res 2005;35:1224–32.
[42] Komnitsas K, Zaharaki D, Perdikatsis V. Geopolymerisation of low calcium ferronickel slags. J Mater Sci 2007;42:3073–82.
[43] Palomo A, Grutzeck MW, Blanco MT. Alkali-activated fly ashes A cement for the future. Cem Concr Res 1999;29:1323–9.